Localization and electron-interaction effects in a two-dimensional metal with strong spin-orbit scattering: Pd films

R. S. Markiewicz and C. J. Rollins
Department of Physics, Northeastern University, Boston, Massachusetts 02115
and Francis Bitter National Magnet Laboratory, Cambridge, Massachusetts 02139
(Received 4 October 1982; revised manuscript received 21 June 1983)

We observe positive, anisotropic, strongly-temperature-dependent magnetoresistance in ultrathin [(6—55)-Å] Pd films. Interpreted in the light of recent theory, we find that localization effects dominate, but that electron-interaction effects are present as well. A strong spin-orbit scattering (symplectic limit) causes the localization-induced magnetoresistance to be positive. The inelastic scattering rate varies as T^2, although its magnitude is considerably larger than expected for electron-electron scattering. In some films we find a low-temperature drooping of the magnetoresistance which cannot be explained in the conventional localization—plus—electron-interaction theory.

I. INTRODUCTION

Recent theories of conductivity in lower-dimensional systems[1–3] have predicted that the resistance R increases with decreasing temperature, diverging as $T\rightarrow 0$. In two dimensions, the predicted logarithmic increase, $R\propto \ln T$, has been observed in Si inversion layers[4–6] and thin metallic and semimetallic films.[7–19] Two separate mechanisms contribute to the logarithmic increase—electron localization[1,3] and many-body effects.[2] Magnetoresistance (MR) and Hall-effect measurements can distinguish between these mechanisms. In Si inversion layers both mechanisms make comparable contributions, and the magnetic studies allow a clear separation of the two effects.[4–6] In metal films localization effects are dominant in producing the MR.[7–19]

We report here the MR of ultrathin Pd films (6—55 Å) for fields up to 14 T and temperatures 1.3—50 K. This wide range of fields and temperatures allows a detailed comparison with the theoretical predictions.

We find that (1) for all films the MR is positive for $T<30$ K and grows rapidly at low temperatures, but (2) the MR is anisotropic, being much larger when the field is applied perpendicular to the film plane. These two facts can be explained by assuming that localization effects are dominant with strong spin-orbit scattering causing the positive MR.[3,20] A more detailed comparison with theory yields the following additional results. (3) The inelastic scattering length varies as T^{-2}, consistent with electron-electron scattering. (4) Magnetic impurity scattering becomes important at low temperatures. (5) The MR anisotropy is well described by the theory of Al'tshuler and Arnov.[21] (6) In some films there is an anomalous dependence of the amplitude of the MR on temperature. At the lowest temperatures the MR may be a factor of 2 smaller than expected from a high-T extrapolation. (7) Electron interaction effects give a weak contribution to the MR ($F\lesssim 0.1$), but produce essentially all of the T dependence of the resistivity at high fields, where localization effects are saturated.

In the following section we shall summarize the various theoretical expressions of MR in two-dimensional (2D) films. In Sec. III we will present our data and in Sec. IV compare it to theory and to other experiments. Section V summarizes our results.

II. THEORY

A. Localization: Orthogonal limit

Hikami, Larkin, and Nagaoka[3] (HLN) have shown that the localization-induced MR is very sensitive to any spin-dependent scattering (spin-orbit or magnetic impurity scattering). While these effects may be small in Si inversion layers and films of light metals, the spin-orbit scattering should be very strong in films made of heavy atoms. For completeness, however, we will briefly summarize the predictions of localization theory when spin-dependent scattering is negligible. Following HLN and Dyson,[22] this limit is called the *orthogonal* limit.

In zero field, localization theory predicts

$$\sigma=\sigma_0+\beta\ln(l_e/l_i)\ , \tag{1}$$

where $\sigma_0^{-1}=R_0$ is the bulk value of the sheet resistance $\beta=e^2/2\pi^2\hbar$, l_e is the elastic scattering length, and l_i is the inelastic scattering length. Generally, $l_i=l_{i0}/T^P$, where P is an exponent characteristic of a particular scattering mechanism, and σ decreases logarithmically with decreasing temperature T. The most probable mechanism for l_i is electron-electron scattering, for which $P=2$ [clean, three-dimensional (3D) limit] or $P=1$ [dirty (2D) limit].[23] A magnetic field acts to destroy localization and there is a negative MR. For the transverse case (field perpendicular to film plane)

$$\Delta\sigma_\perp(H,T)=\beta[f(l_H^2/L^2)-f(l_H^2/2l_e^2)]\ . \tag{2}$$

Here $f(x)=\psi(x+1/2)-\ln(x)$, ψ is the digamma function, $L=(2l_el_i)^{1/2}$ is the Thouless length, and $l_H=(\hbar c/eH)^{1/2}$ is a magnetic length.

If the field is applied parallel to the film surface, the

electronic states can no longer be described in terms of Landau levels, and the term $\Delta\sigma_\perp$ is absent. However, Al'tshuler and Aronov[21] have shown that there is still a negative MR,

$$\Delta\sigma_{||}(H,T)=\beta\left[\ln\left[1+\frac{t^2L^2}{12l_H^4}\right]\right]. \tag{3}$$

Here t is the film thickness. In low fields, both Eqs. (2) and (3) predict MR varying quadratically with H, but $\Delta\sigma_{||}/\Delta\sigma_\perp=2t^2/L^2\ll 1$ at low T.

B. Localization theory: Symplectic limit

HLN generalize the above theory to include spin-orbit scattering (with corresponding scattering length l_{so}) and magnetic impurity scattering (l_s). Localization effects are absent in the *unitary* case ($l_s\ll l_i,l_{so}$)—the conductance is independent of H,T. In the strong spin-orbit scattering, or *symplectic* limit ($l_{so}\ll l_s,l_i$) localization effects occur, but *with opposite sign*—that is, positive MR and zero-field resistance which decreases with decreasing T. In particular,

$$\sigma=\sigma_0-\frac{\beta}{2}\ln\left[\frac{l_e}{l_{sym}}\right], \tag{4}$$

$$\Delta\sigma_\perp(H,T)=-\frac{\beta}{2}f\left[\frac{l_H^2}{2l_el_{sym}}\right], \tag{5}$$

$$\Delta\sigma_{||}(H,T)=-\frac{\beta}{2}\ln\left[1+\frac{t^2l_el_{sym}}{6l_H^4}\right], \tag{6}$$

where $l_{sym}^{-1}=l_i^{-1}+2l_s^{-1}$.

C. Localization theory: General case

While our films are close to the symplectic limit, we have fit our data to the full theory of HLN, generalized to allow for (i) arbitrary values of l_i,l_s,l_{so}, (ii) anisotropy of l_{so} [$l_{so}^{-1}=2(l_{so}^x)^{-1}+(l_{so}^z)^{-1}$, where the z axis is perpendicular to the film plane], and (iii) Zeeman splitting of the electron states.[24] In this case, Eqs. (1)–(3) should be replaced by

$$\sigma=\sigma_0+\frac{\beta}{2}\left[\ln\left[\frac{l_e}{l_1}\right]+\ln\left[\frac{l_e}{l_2}\right]+\ln\left[\frac{l_e}{l_3}-\frac{l_e}{l_4}\right]-\ln\left[\frac{l_e}{l_3}+\frac{l_e}{l_4}\right]\right], \tag{7}$$

$$\Delta\sigma_\perp(H,T)=\beta\left\{f\left[\frac{l_H^2}{2l_el_1}\right]-f\left[\frac{l_H^2}{2l_e^2}\right]+\frac{1}{2(1-\gamma_\perp)^{1/2}}f\left[\frac{l_H^2}{2l_e}\left[\frac{1}{l_{3_\perp}}-(1-\gamma_\perp)^{1/2}\frac{1}{l_{4_\perp}}\right]\right]\right.$$
$$\left.-\frac{1}{2(1-\gamma_\perp)^{1/2}}f\left[\frac{l_H^2}{2l_e}\left[\frac{1}{l_{3_\perp}}+(1-\gamma_\perp)^{1/2}\frac{1}{l_{4_\perp}}\right]\right]\right\}, \tag{8}$$

$$\sigma+\Delta\sigma_{||}=\sigma_0+\frac{\beta}{2}\left[\ln\left[\frac{l_e}{l_1}+\frac{t^2l_e^2}{6l_H^4}\right]+\ln\left[\frac{l_e}{l_2}+\frac{t^2l_e^2}{6l_H^4}\right]-2\ln\left[1+\frac{t^2l_e^2}{6l_H^4}\right]\right.$$
$$\left.+\frac{1}{(1-\gamma)^{1/2}}\ln\left[\frac{l_e}{l_3}-\frac{l_e}{l_4}(1-\gamma)^{1/2}+\frac{t^2l_e^2}{6l_H^4}\right]-\frac{1}{(1-\gamma)^{1/2}}\ln\left[\frac{l_e}{l_3}+\frac{l_e}{l_4}(1-\gamma)^{1/2}+\frac{t^2l_e^2}{6l_H^4}\right]\right]. \tag{9}$$

(For $\Delta\sigma_{||}$, cf. Ref. 10.) Here

$$l_1^{-1}=l_i^{-1}+2\left[\frac{l_s^{-1}}{3}+(l_{so}^z)^{-1}+(l_{so}^x)^{-1}\right], \tag{10}$$

$$l_2^{-1}=l_i^{-1}+2\left[\frac{l_s^{-1}}{3}+2(l_{so}^x)^{-1}\right], \tag{11}$$

$$l_3^{-1}=l_i^{-1}+\left[\tfrac{4}{3}l_s^{-1}+(l_{so}^x)^{-1}+(l_{so}^z)^{-1}\right], \tag{12}$$

$$l_4^{-1}=\tfrac{2}{3}l_s^{-1}-(l_{so}^x)^{-1}-(l_{so}^z)^{-1}. \tag{13}$$

The correction due to Zeeman splitting, $\gamma=(hl_4/\hbar v_F)^2$, is expected to be small (the HLN results follow when $\gamma\to 0$); v_F is the electronic Fermi velocity, $h=g_e\mu_BH$, with g_e the electronic g factor and μ_B the Bohr magneton, and $l_{3\perp}$, $l_{4\perp}$, and $\gamma_\perp$ differ from l_3, l_4, and γ in that l_{so}^z is replaced everywhere by l_{so}^x. Additional corrections, due to anisotropy of l_s and the possibility that l_e is not $\ll l_s,l_{so},l_i\gg$, are discussed in Refs. 3 and 24.

D. Many-electron effects

Interactions among electrons also modify the 2D conductance in ways which are similar to localization corrections. These many-electron effects are also sensitive to spin-orbit and magnetic impurity scattering, but the expressions for sample conductance have not been worked out in as much detail as for localization effects. In zero field the $\ln T$ correction to the conductance has the form[2,25–27]

$$\sigma'=\beta(1-\alpha F)\ln(k_BTl_e/v_F\hbar). \tag{14}$$

The parameter F measures the importance of screening with $F=0$ in the strong screening limit ($2k_F\gg\kappa$, where

k_F is the 2D Fermi wave vector and κ is the inverse screening length) and $F=1$ when screening is weak ($2k_F \ll \kappa$).

Two separate mechanisms contribute to the interaction effect. One is due to many-body corrections to the particle-hole propagator,[27] the other to corrections to the particle-particle propagator.[25,26] The latter corrections are renormalized[27,28] by a factor $\lambda=1/[1+0.5F \times \ln(E_F/T)]$, where $\ln(E_F/T)\simeq 10$ for our Pd films. If spin-orbit coupling is negligible,[25] the combined effect of these two terms is $\alpha=1+0.5\lambda$. In the symplectic limit[26] $\alpha=(1+2\lambda)/4$.

In a magnetic field both mechanisms contribute a positive magnetoresistance. The particle-particle corrections correspond to orbital effects[25,28] and hence should have an anisotropy similar to the localization effects. The particle-hole corrections, on the other hand, depend on spin splitting of the electrons,[27] and hence should be independent of field orientation. However, spin-orbit scattering effectively mixes spin-up and spin-down states, so that this MR contribution is absent in the symplectic limit.[26] Since the remaining terms are reduced by a factor λ, it is expected that interaction effects should make a negligible contribution to the MR. Since this is so, and since the field dependence has not been calculated in detail when spin-orbit scattering is strong, we approximate the interaction-induced MR by the Lee-Ramakrishnan[27] expression

$$\Delta\sigma'(H,T)=-\frac{\beta F}{2}g(h/k_BT)\ , \tag{15}$$

where

$$g(x)=\int_0^\infty d\Omega \ln\left|1-\frac{x^2}{\Omega^2}\right|\frac{d^2}{d\Omega^2}\left[\frac{\Omega}{e^\Omega-1}\right]\ .$$

As $x \gg 1$, $g \to \ln(x/1.3)$, while $x \ll 1$, $g=0.0914x^2$. In Appendix A we show that this expression approximates the field dependence for the strong spin-orbit-coupling case as well, but may *overestimate F*.

Al'tshuler and Aronov[21] have proposed an additional contribution to the many-electron MR (this one negative) for H parallel to the film plane, but we have seen no evidence of this effect. Also, since our films are in the $\omega_c\tau \ll 1$ limit, we need not consider the high-field theory of Houghton *et al.*[29]

III. EXPERIMENTAL RESULTS

A. Films

Thin films of Pd are prepared by sputter deposition onto single-crystal Si substrates at room temperature. Film thickness is determined by a quartz-thickness monitor calibrated with electron-microscopic measurements on similar Pt films.[11] Details of the preparation techniques and a study of the electrochemical properties of these films have been published separately.[30]

For Pd films deposited on Si at room temperature a silicide is formed at the interface.[31,32] Since the silicides are themselves good conductors we should still expect to see localization effects, but it is important to understand the nature of the silicides to interpret our data. Evidence from a variety of sources[32] suggest that the thinnest films ($t \leq 5$ Å) are a poorly characterized phase of approximate composition PdSi (this is *not* the same as the PdSi which can be formed by high-temperature annealing). Films from $\sim$5–20 Å in thickness appear to be uniformly Pd_2Si. If more material is added, it remains pure Pd with a relatively sharp interface. (In this paper, all quoted thicknesses are in Å of Pd deposited; the Pd_2Si phase is actually about 50% thicker.) We expect the above results to be applicable to our films. However, slow changes of room-temperature resistivity and electrochemical properties of samples kept at room temperature suggest that our silicide layers may be relatively thicker. Films with $t < 30$ Å also showed evidence of long-term diffusion. We could not make Ohmic contacts which would withstand cycling to low T when these samples were freshly prepared—suggesting discontinuous metal islands. Such contacts could be made after the film had aged for several months.

The above analysis has been confirmed by recent low-temperature measurements. Pd_2Si goes superconducting at $T_c \cong 0.25$–0.5 K (depending on the film). In our 30-Å film, the resistance goes to zero at this temperature, suggesting that this film is nearly pure Pd_2Si. In a 50-Å film there is a residual nonzero resistivity below the superconducting transition. This is consistent with the film being bilayer—Pd and Pd_2Si. Because of thickness variations the proximity effect drives some fraction of the Pd_2Si normal. In contrast a 6-Å film shows no trace of superconductivity, showing that this is a different phase from Pd_2Si. These results will be described in more detail elsewhere.[33]

B. Magnetoresistance

We have observed MR in a variety of samples of thickness ranging from 6 to 55 Å, in a temperature range from 1.3 to 50 K, and in magnetic fields up to 14 T applied either perpendicular or parallel to the film plane. For detailed comparison to theory, we measured three films throughout the full field and temperature range for both field geometries. These films had measured thicknesses of 55, 30–32, and 6–7 Å, and hence should represent bilayer, Pd_2Si, and PdSi phases, respectively. Data from other films were always consistent with these, and, for comparison, other fits to less complete data sets are also included in Table I.

Resistivity was measured by a four-point-probe technique using silver epoxy contacts to the sample. The results were corrected for sample edge effects by solving for the 2D potential distribution in a rectangle. For $T \leq 4.2$ K, the sample was immersed directly in liquid He and the temperature was controlled by varying the pressure above the liquid. For higher temperatures, the sample was cooled with a He exchange gas, with temperature measured at zero field by a calibrated carbon-glass thermometer. Temperature was controlled by a heater coil surrounding the sample area. Constant temperature was maintained through a feedback loop using a $SrTiO_3$ capa-

TABLE I. Film parameters. All fits use $P=2$. Errors are determined in two ways. The parameters whose errors are listed in parentheses are chosen to have fixed values, while the remaining parameters are varied to minimize $\chi^2 \equiv \sum[\Delta\sigma(\text{theory})-\Delta\sigma(\text{expt.})]^2$. Errors given as ± are then estimated by the fitting routine, while the numbers in parentheses indicate the range of values for which χ^2 is less than twice its minimum value. All parameters should have an additional uncertainty of ~30% from inaccuracies in data reproducibility and variation of subsidiary parameters.

(a) Localization lengths

t (Å) As deposited	From MR anisotropy	$R_0(\Omega)$	l_e (Å)	L_0 (Å)	l_s (μm)	l_{so} (Å)	l^x_{so}/l^z_{so}	
(i) Full data sets								
(1) 55	58	172	22	4200±100	1.13±0.04	75 (≤180)	1 (≤4)	
(2) 30–32	40	650	9.5	4800±100	500	300 (≤2000)	12 (5–20)	
(30 6–7	44	1930	16[a]	3500±400	0.35±0.04	70 (≤200)	1 (≤10)	
(ii) Partial sets								
t range	Parameter set			Changed values				
55 $H\|\|$, $T>4$ K	1	171	22	4000	8[b]			
55 $H\|\|$, $T>4$ K	1	140	27	6000±1400	400[b]			
50 $H\perp$, $T<4$ K $H\|\|$, $T>4$ K	1	160	24	4400	24			
30 $H\perp$, $T<4$ K	2	649	9.5	6000	60	250	1	two fits
$H\|\|$				5800	40	200	20	
30 $H\perp$	2	700	9	4600	9.5		20	two fits
				4500	9.5		26	
15 $H\perp$	2	1730	8	3700	10			
30 (glass $H\perp$ substrate)	1	147	45	14000±5000	0.4			

(b) Other parameters

		Localization parameters			Electron interaction		
t (Å)	$\bar{\beta}$	$g_e/2$	β_1	T_c	F	$g_e/2$	$\bar{\beta}(1-F/2)$
(i) Full data sets							
(1) 55	2.1 (1.7–2.6)	0.7 (≤2)	3.1±0.1	0.06 (0.01–0.26)	0.014±0.004	14±7	(0–6)[c]
(2) 30–32	2.0±0.1	0 (≤2)	3.5±0.2	0.04±0.01	0.054±0.005	10±2	2.1
(3) 6–7	0.91 (0.6–1.8)	1.7 (≤4)	3.4±0.9	0.07 (≤0.7)	0.052±0.017	6±3	0.9
(ii) Partial sets							
55	2.0		9[b]		0.10		(1–4)[c]
55	1.5		4.7[b]	0.2[b]	0.01		
50	2.2		3.0				2.8
30	0.8	0.5	0		0.074	11±5	0.9
	0.74	0.6	0		0.26	5	
30	1.4		0				0.5
	1.2		0		0.18		
15	1.0						1.8
30 (glass)	1.4		5.1	0.07	0		0.7

[a]Assumes $t=6.5$ Å.
[b]Large uncertainty due to poor T range for fit.
[c]See Appendix C.

citance thermometer. For the 6-Å film we attempted to control the temperature using the carbon-glass resistor, but its MR was large enough to cause errors in the measured Pd MR. This was corrected by subtracting out the zero-field resistance change due to T variations.[34]

The data were compared to theoretical expressions (8), (9), and (15). The results of least-squares fits are shown in Figs. 1—3 with parameters listed in Table I. Table I also lists the residual resistivity R_0 of our films. The theoretical expressions, Eqs. (1)—(15) are calculated by a perturbation theory with a small parameter $\hbar/E_F\tau$ which can be rewritten as $R_0/12.95$ kΩ (Appendix A). Since this parameter is less than 0.2 in all of our films, the perturbation theory results should provide an adequate description.

We estimate an average, overall uncertainty of ~30% in each parameter of Table I with some exceptions to be noted shortly. The MR data are reproducible to about 15% on warming to room temperature and recooling. (The total resistance varies by only about 1%, but the MR is generally less than 1% of R_0.) This thermal cycling change shows up as a mismatch between the high-T data taken in an exchange gas, and the low-T data, directly immersed in liquid He. The mismatch shows up both as a jump in the zero-field resistivity and a change in the amplitude of the MR. We adjust the data by scaling the amplitudes of the low-temperature data, since this subgroup corresponds to the anomalous zero-field resistivity. This adds primarily to the uncertainties in $\bar{\beta}$ and t. For the 30-Å film we took all of the data in the exchange gas, thus eliminating part of this problem. (The sample still had to be warmed up to change from perpendicular to parallel fields.)

A check of our reproducibility is given by the analysis of the incomplete data sets listed in Table I. Deviations generally occur from attempting to measure a parameter with an inappropriate data set—e.g., l_s and β_1 are most prominent in the low-T data, whereas L_0 is best determined at higher T, and the $\vec{H}||$ data are in general less sensitive to the individual parameters. (The insensitivity of the data for these incomplete sets is often shown by

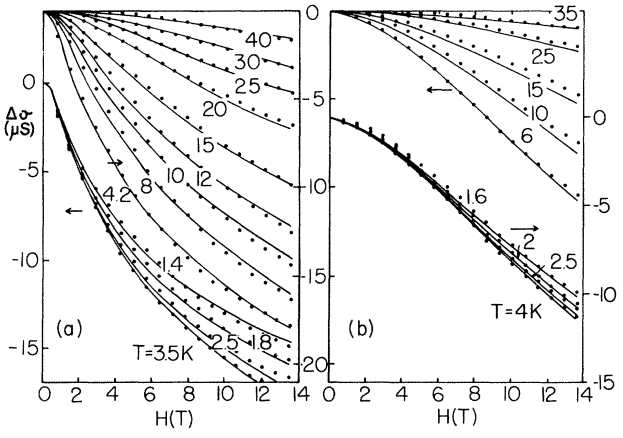

FIG. 1. Transverse MR of 55-Å Pd film. Dots indicate data and solid curves indicate the theory using parameters of Table I. (a) $H\perp$ to film, (b) $H||$ to film.

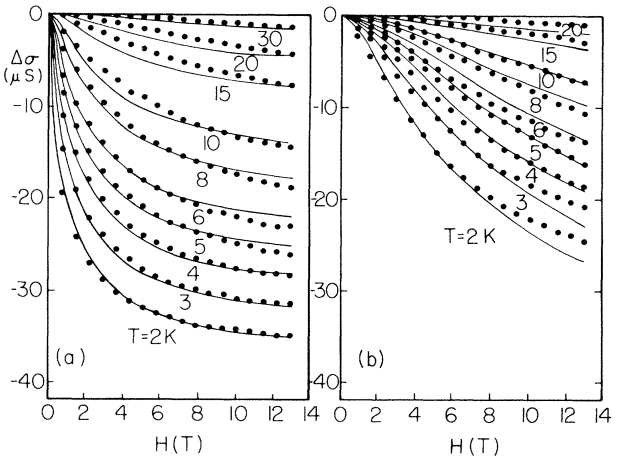

FIG. 2. Transverse MR of (30—32)-Å Pd film. Dots indicate data and solid curves indicate the theory using parameters of Table I. (a) $\vec{H}\perp$ to film and (b) $\vec{H}||$ to film.

poor convergence of the fitting routine, with two or more parameters varying over a wide range with negligible improvement of the fit.)

In the remainder of this section and the following section we discuss the individual parameters of the fit. This section is more concerned with how the parameters affect the overall fit, while the following section compares the values obtained to theory.

The data were fit using a nonlinear least-squares-fitting routine; the final parameters were found by simultaneously fitting the parallel and perpendicular data at all temperatures. Certain parameters were not allowed to vary, but were assigned particular values. Thus the band parameters $m \simeq m_0$ (the free-electron mass) and $v_F \simeq 5.3 \times 10^7$ cm/sec (Appendix B), were estimated from the parameters of bulk Pd. The estimate is only approximate, since Pd is a compensated metal, but no band-

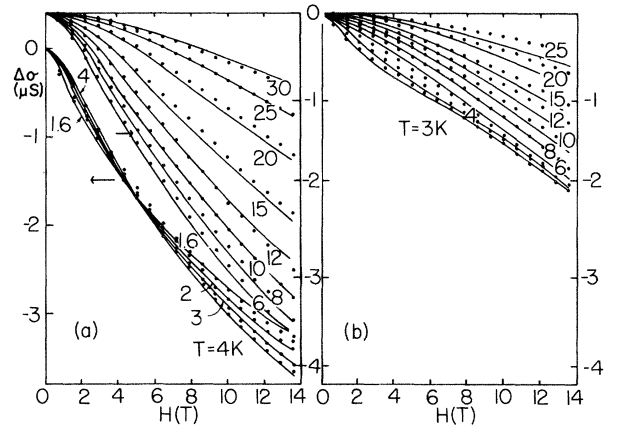

FIG. 3. Transverse MR of (6—7)-Å Pd film. Dots indicate data and solid curves indicate theory using parameters of Table I. (a) $\vec{H}\perp$ to film and (b) $\vec{H}||$ to film. In (a) note the experimental MR curves for $T \leq 4$ K invert their order at $H \simeq 5$ T, and that this behavior is matched in the theory.

TABLE II. Revised parameters found by requiring l_{so} and l_e to have the appropriate ratio.

t (Å)	l_e (Å)	l_{so} (Å)	l_{i0} (μm)	l_s (μm)	$g_e/2$	$\rho_\infty l_\infty$ (Ω Å^2)
55	6.6	230	130	3.9	0.2	60000
30–32	9.0	320	130	500	0	190000
6–7	5.6	200	110	1.0	0.6	70000

structure effects are accounted for in the theory. These parameters affect only the value of the g factors.

The parameter l_e is determined from the residual resistivity, using $R_0=\rho_\infty l_\infty/l_e t$, where the material parameter[35] $\rho_\infty l_\infty$ is taken[36] as 2×10^5 Ω Å^2. From Eqs. (8) and (9), the MR depends mainly on the products[37] $l_e l_i, l_e l_s, l_e l_{so}$, so that any change in the value of l_e is compensated for by a corresponding change in these other values. This method of fixing l_e is subject to three sources of error. Firstly, the value of $\rho_\infty l_\infty$ may not be appropriate for our films—the literature values[36] vary by a factor of 3. Secondly, if the films are nonuniform in thickness, or have pinholes, the value of l_e entering R_0 may be different from that relevant to localization theory. Finally, since the carriers of Pd are both electrons and holes with several different effective masses, the averaging of l_e may be different for R_0 and for localization theory. We will see below that a smaller value of l_e would appear to be necessary to explain our localization results (due most probably to a smaller value of $\rho_\infty l_\infty$—Table II).

Owing to the large number of parameters care had to be taken to ensure that the fitting routine was finding the best minimum. The procedure finally decided on was as follows. A scaling analysis was used to determine P and various subsets of the data were used to generate initial estimates of the parameters. (Having fit the perpendicular field data, a good fit to the parallel data could generally be obtained by varying only t. The reverse was not true, however, since most of the parallel data is in the low-field limit, when the theory is less sensitive to individual parameters.) The most sensitive parameters were found to be l_i, l_s, F, g_e (many-electron), and β_1. These were varied to find the best fit to all of the data, keeping the other parameters constant. Finally, the other parameters were allowed to vary as well, to get the final fit. To explore the range of possible values for, e.g., l_{so}, this parameter was set to a new value and the five "sensitive" parameters varied to find the new minimum.

The parameter P was not varied directly, but l_i was chosen to have the form $L_i^{-1}=aT+bT^2$, which is expected for electron-electron scattering and has been observed in Si inversion layers.[38] We obtained our best fits by setting $a=0$, although observation of nonzero a is obscured at low T by the finite value of l_s and by interaction terms [Eq. (15)]. A technique which was proven useful for determining the T dependence of the MR without detailed fitting is to use the scaling properties of the various theoretical expressions. Since the different contributions scale differently, this technique is most valuable when one contribution dominates, as in the 55-Å films (Fig. 4). In the symplectic limit, $\Delta\sigma_\perp$ [Eq. (5)] is a function only of the ratio $H/(A+T^P)$, where $A=2l_{i0}/l_s$. For a fixed value of $\Delta\sigma_\perp$, we can determine what value of H is required to attain that $\Delta\sigma_\perp$ at different temperatures. Figure 4(a) shows a plot of the resulting curves of $H(T)$, the "level curves" of the 55-Å film for $\Delta\sigma_\perp$. All curves are linear when plotted versus T^2, with a common intercept at $T^2=-A$. This figure employs the value of $A=71$ found from more detailed analysis (Table I). We immediately see that many-electron effects (for which $P=1, A=0$) are negligible. Furthermore, the MR for H parallel to the film plane should scale as $H^2/(A+T^P)$, as we find in Fig. 4(b), using the same values of A,P. This same scaling on the (30–32)-Å film shows a T^2 contribution at high T, and T^1 at low T, which detailed curve fitting shows to be due to many-electron effects. Because of many-electron effects and the large value of A (small l_s), the scaling analysis of the (6–7)-Å film could not clearly distinguish T vs T^2.

The data of Fig. 4 contain more information. Since each line corresponds to a fixed value of $\Delta\sigma$, we can plot $\Delta\sigma_\perp$ versus the slope of the curves, $H/(A+T^2)$, as in Fig. 5. This curve represents the best approximation of the data to the symplectic limit and can be fit to Eq. (5) with only two independent parameters β and l_s. Figure 5 shows that choosing β equal to twice its theoretical value gives a much improved fit. Such a conclusion is confirmed by the more detailed analysis (Table I); the advantage of the present analysis is that only a single extra parameter (l_s) needs to be introduced.

In Fig. 4 the MR at low T is seen to deviate from the

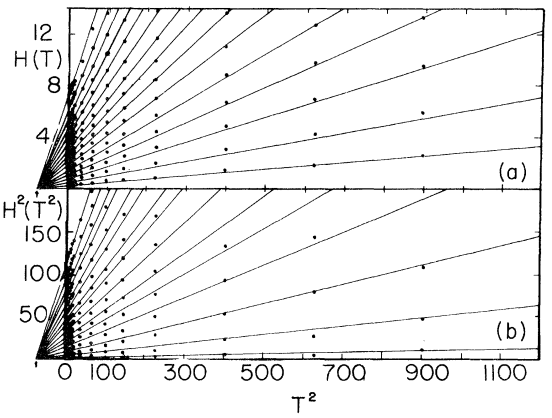

FIG. 4. Level curves of 55-Å Pd film. Dots indicate data and solid lines indicate theory. Each line refers to a single value of MR, plotting the field needed to produce the value of $\Delta\sigma$ as a function of temperature. (Actual values of $\Delta\sigma$ are shown in Fig. 5.) (a) $\vec{H}\perp$ to film, (b) $\vec{H}\|$ to film.

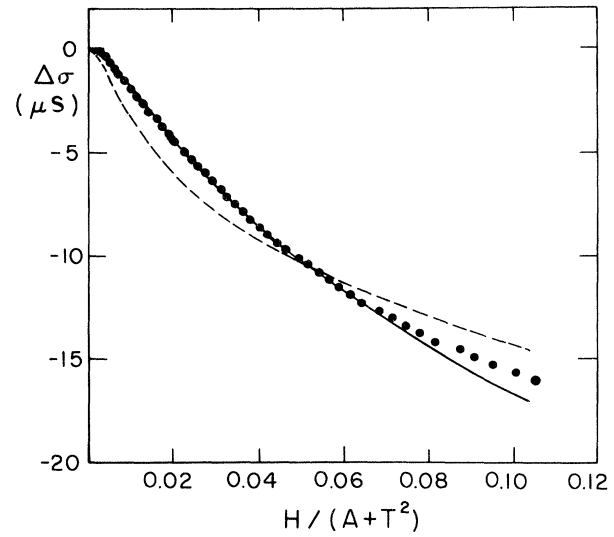

FIG. 5. MR of 55-Å Pd film ($\vec{H}\perp$ to film), plotting $\Delta\sigma$ vs the slopes obtained in Fig. 4. Dots indicate data. Lines are best fit assuming either amplitude of MR has the correct theoretical values (dashed line) or that it is twice as large as predicted (solid line). As explained in the text only one parameter (l_s) is varied in the fit.

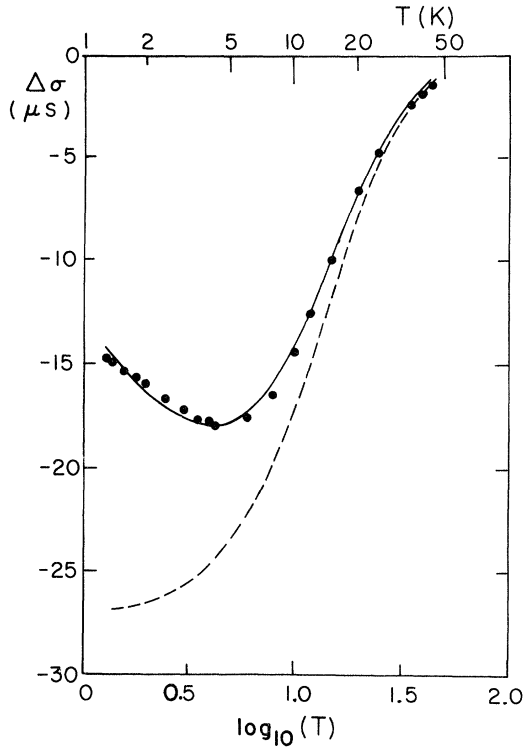

FIG. 6. Magnetoresistance of 55-Å Pd film at fixed field ($H=13.5$ T, $\vec{H}\perp$ to film) as a function of temperature. Solid line is the fit using parameters of Table I; dashed line indicates the same theory but neglecting the drooping ($\beta_1\to 0$.)

scaling prediction. This deviation, replotted in Fig. 6, cannot be explained on the basis of the theoretical expressions discussed so far. These expressions give a MR which is monotonic in T at fixed H, whereas the data for the 55-Å and (6—7)-Å films show a considerable drooping at low T. In order to fit this data, we have had to find a means of parametrizing this drooping. We have found that the data can be adequately described by a function introduced by Larkin[39] in a study of the interaction of localization and superconducting fluctuations above T_c. The theory amounts to making the amplitude of the MR temperature dependent,

$$\beta\to\beta(T)=\frac{e^2}{2\pi^2 h}\left\{\bar{\beta}-\beta_1\gamma_L\left[\ln\left[\frac{T}{T_c}\right]\right]\right\}. \tag{16}$$

The theory introduces two parameters β_1 and T_c, and γ_L is a function tabulated in Ref. 39, where $\gamma_L(x)\to\pi^2/6x^2$ for $T\gg T_c$. The parameter β_1 should be -1 in Larkin's theory. The significance of this parametrization will be further discussed in the following section, although we hasten to point out that there are serious difficulties in connecting it with a superconducting transition (in particular, the fact that β_1 is field independent to 14 T). However, Figs. 1, 3, and 6 show that Eq. (16) provides an adequate parametrization of this "drooping" effect.

IV. DISCUSSION OF RESULTS

Figures 1—3 show that there is a considerable difference between the MR of the 30-Å film and that of other films. This appears to be due mainly to a very small value of l_s in this film. However, the shape of the MR in the 30-Å film is similar to that expected from interaction effects; this leads to a much greater uncertainty in parameter values—for instance, fits could also be found for $F\simeq 0.2$. An examination of Table I shows that the values of β_1 and spin-orbit anisotropy could not be accurately determined for the 30-Å films.

A. Magnetoresistance parameters

$\bar{\beta}$. The theory described above predicts that $\bar{\beta}=\beta/(e^2/2\pi^2\hbar)$ is simply equal to 1. While we expect some scatter in the data because the value depends on an absolute calibration of the resistance, our results appear to vary between 1 and 2. A similar situation occurs in Si inversion layers, where the $\bar{\beta}$ variation is presumed to arise from the several valleys of the conduction electrons.[25,40] If the valleys interact weakly, their localization effects are additive, and $\bar{\beta}=n$, the number of occupied valleys. If valley-valley scattering is strong, $\bar{\beta}$ is reduced to 1. A similar explanation may hold in Pd, due to either band-structure effects (both electron and hole orbits are possible), or the presence of two film layers, Pd and silicide, in the thicker films.

The nearly constant value of $\bar{\beta}\simeq 1-2$ for all samples studied confirms that the MR is due to a localization-interaction effect, and not to some bulk mechanism. For a bulk effect, one would expect $\Delta R\propto R_0$, so $\Delta\sigma\simeq-\Delta R/R_0^2\propto 1/R_0$, or $\bar{\beta}\propto\Delta\sigma$ would vary by a factor greater than 10. The remaining variation observed (about

a factor of 2) appears to be a genuine sample-dependent effect: If different 30-Å films are compared at a fixed temperature, their net MR varies from sample to sample, proportional to the values of $\bar{\beta}$.

l_{so}. In the symplectic limit, Eqs. (4)—(6), the MR is independent of l_{so}. We find that our fits are insensitive to this value, having a weak minimum in χ^2 at the value listed in Table I. The table also lists the maximum value of l_{so} compatible with the data—defined as that value for which the χ^2 of the fit (allowing other parameters to vary) is increased by a factor of 2.

Theoretically, $l_{so} \simeq l_e/\epsilon$ with $\epsilon \propto Z^4$ (Z is the atomic number). The data of Meservey and Tedrow on other metals[41] indicate $\epsilon^{-1} \simeq 35$ for Pd. Our data, in general, show a considerably smaller value of ϵ. We suggest that this is evidence that we have chosen values of l_e which are too large. Since our data gives the product $l_e l_{so}$, we can find consistent values of l_e, l_{so} by assuming $\epsilon^{-1}=35$. This is done in Table II, which also lists the revised values for l_{i0}, l_s, and g_e. (Note that this is *not* a refitting of the data—merely a rescaling of the previous values due to the new choice of l_e.) For the new parameter values l_i is approximately constant. From R_0 and the new l_e, we calculate the values of $\rho_\infty l_\infty$ listed in Table II. The values of $\rho_\infty l_\infty$ fall within the range of previously reported values.[36]

l_{so}^x. In the 2D limit the quantum-size effect quenches the transverse components of spin-orbit scattering,[3,24] leaving only l_{so}^z finite, whereas in three-dimensions all components are approximately equal. Earlier experiments[41] suggest that these effects can be strong when $t < 100$ Å. We see possible evidence for this only for our 30-Å films, although we cannot rule out a relatively small anisotropy of $\sim < 5$ in the other films.

l_i. All films have comparable values of $l_i \simeq (100\text{—}200\ \mu\text{m})/T^2$, differing by only a factor of 2 between Pd and Pd_2Si. The T dependence is that expected for (clean) electron-electron scattering. These values can be contrasted with the effect of electron-electron scattering on bulk resistivity. For Pd, it is found[42] that $\rho_{ee} \simeq 3.3 \times 10^{-11} T^2$ Ω cm, leading to $l_{ee} \simeq (6000\ \mu\text{m})/T^2$. In Pd_2Si, l_{ee} is expected to be much larger, and has not been measured.

The reason for these differences is clear. The ordinary s-s electron scattering does not contribute to bulk resistivity in lowest order. The larger value of ρ_{ee} in Pd is produced by s-d scattering, which is absent in Pd_2Si, since the d bands are filled. In contrast, any electron-electron scattering serves to delocalize an electron, leading to significantly smaller values of l_i.

l_s. There is considerable spread in the values of l_s listed in Table I. Some of this spread is real—Figs. 1—3 show that the 30-Å film has a considerably stronger field dependence at low T due to a larger value of l_s. Part of the spread is due to the fact that the measure of l_s is rather indirect. Figure 4 shows that it is found essentially as a zero-field intercept and this extrapolation can have large uncertainties even when there are no competing effects. Nevertheless, the values are all $\sim \geq 1\ \mu$m, indicating weak effects. For instance, if the magnetic impurity were iron, comparison of Table II data with results[43] on bulk Pd:Fe would suggest a concentration of about 400 ppm for the smallest l_s (other impurities yield comparable values). This is larger than the concentration in our starting Pd, but Fe or Cr are not uncommon contaminants in a sputtering system.

There is presently some question as to the theoretical interpretation of l_s. The theory of HLN took magnetic impurity scattering into account in lowest order only. At low T, the Kondo effect acts to quench the magnetic moment, while a high field aligns the impurity spins and hence inhibits spin-flip scattering.[44] Further analysis of this term must await more detailed theoretical understanding. In Appendix C we suggest that our observation of a constant l_s is consistent with the Kondo effect.

Many-electron parameters. The presence of many-electron effects is most clearly shown in the 6-Å film at low T. Figure 7 shows a decomposition of the MR into localization and many-electron contributions. The parallel MR shows a clear knee when the many-electron term reaches its high-field limit. The knee occurs when $g_e \mu_B H = 2\pi k_B T$, giving $g_e \simeq 14$, in agreement with Table I. The small values of F we observe are consistent with other investigations, in which many-electron effects were not detected.[8,10,15] The values of the g factor are much larger than expected, possibly due to a band-structure or many-electron effect. The relatively low-field saturation of the effect could be consistent with orbital contributions (Appendix A), but then it is not clear why the effect appears to be isotropic.

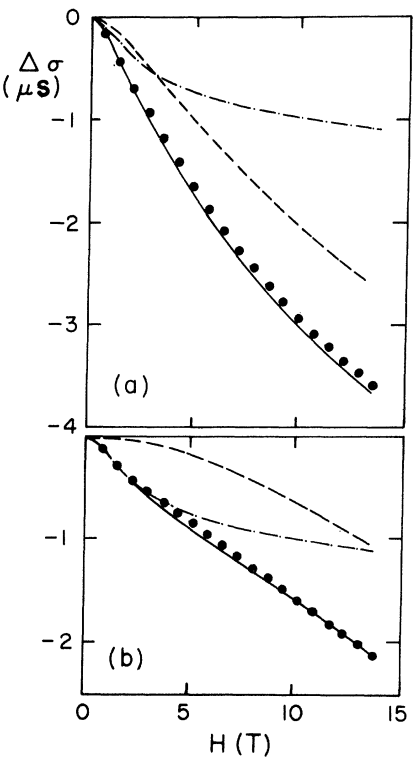

FIG. 7. MR of (6—7)-Å Pd film at 3 K showing decomposition of theoretical curves (solid lines) into localization (dashed) and many-electron (dotted-dashed) contributions. (a) $\vec{H} \perp$ to film and (b) $\vec{H} \parallel$ to film. Data of (b) show a prominent knee at $H \simeq 2$ T, the field at which the many-electron effect saturates.

g_e *(localization).* The strong spin-orbit scattering mixes up and down spins, so the splitting effect proposed by Maekawa and Fukuyama[24] is expected to be weak. The fits to MR generally show a slightly improved fit by including this effect with values $g_e \simeq 2$. This value of g_e is what would be expected for bulk Pd, and it is not clear why it is so different from the value found from many-electron effects.

Drooping of MR at low T. We were able to find a simple parametrization of the drooping (Fig. 6) with Eq. (16), taken from Larkin's work on superconducting fluctuations.[39] The films showed similar values of the two parameters β_1 and T_c although the data were not very sensitive to T_c (Table I). Superconducting fluctuations do not, however, appear to be the correct explanation of the effect. The sign of the observed effect is opposite that of Larkin's theory, and its amplitude is field independent up to 13.5 T. We have observed ordinary superconductivity in the thicker films with $T_c \sim 0.25$–0.5 K. The MR associated with this superconductivity appears to be a different effect, negligible for $T > 1$ K and completely quenched by fields greater than $2T$.

We believe that the drooping may be related to a T dependence of the anisotropy $\xi = l_{so}^z / l_{so}^x$. If ξ vanishes as $T \to 0$ (a crossover from 3D to 2D spin-orbit coupling), effects very similar to the drooping can be produced. This idea will be further developed in a future publication.[33]

t. The ratio of parallel to perpendicular MR should give a sensitive measure of film thickness t, and we find good agreement in both of the thicker films. We should point out, however, that there is some uncertainty about the expected values for t. The quoted values are for a pure-Pd layer, whereas the silicide thickness is about 50% greater. Since about 10—30 Å are probably converted to silicide, the actual t could be as much as 15 Å greater than the deposited thickness.

For the (6—7)-Å film, there is clearly some discrepancy. The use of parameters comparable to the other films, but $t \simeq 6$—10 Å, gives a parallel MR much smaller than we observe. Part of the explanation of the large $\Delta\sigma_{||}$ may be that the thickness of the metallized region is considerably larger than the as-deposited Pd thickness. Narusawa *et al.*[32] find that for sputtered Pd less than 4.5-Å thick, Pd_2Si does not form, but a more Si-rich phase (of composition PdSi) is formed. As noted earlier, Ohmic contacts could not be made on a freshly prepared film. This suggests that the fresh surface is discontinuous, or at least nonmetallic,[45] and becomes metallized only after a slow diffusion process. Whether such a process can metallize ~ 50 Å of material is another question. It may be that in such thin films quantum-size effects enhance $\Delta\sigma_{||}$.

High-T MR. Above 40 K, the MR becomes small enough to be hard to measure. However, in the 55-Å film we find a small negative contribution above 30 K, appearing initially at low fields and extending to higher fields at higher T. Its origin is not at present understood, but is a sufficiently small effect that it is not likely to significantly perturb our other parameters. The high-T data in Figs. 1—3 all tend to be smaller than expected, which could be related either to this negative MR or to a stronger T dependence for l_i (as would be expected from electron-phonon scattering).

Glass substrate. We include in Table I some preliminary data on Pd sputtered onto a glass substrate, which had been cleaned by plasma etching. In this case there will be no silicide formation. The following differences are noted: l_e, and correspondingly L_0, are considerably larger, and β_1 seems much larger—the drooping of the MR is much more prominent.

B. T dependence of resistivity

So far, we have analyzed the MR and neglected the T dependence of σ in zero field. This is *not* expected to be simply proportional to $\ln T$, since the localization effects saturated when l_i is comparable to l_s. The analysis is greatly simplified by studying the T dependence of σ *at the highest fields* studied. In this case the localization effects are essentially proportional to $\ln H$ and *independent of* T. This is not strictly true, since at low T the Larkin-type correction (β_1) is still T dependent, while at high T (< 10 K) the data are not in the high-field limit, but the residual T dependence is weak and can be accounted for using the localization parameters of Table I. The remaining T dependence should be due entirely to the field-independent interaction terms [Eq. (14)],

$$\sigma = \frac{1}{R_0} + \beta \left[1 - \frac{F}{2} \right] \ln T \, . \tag{17}$$

Figure 8 clearly shows the expected $\ln T$ dependence in

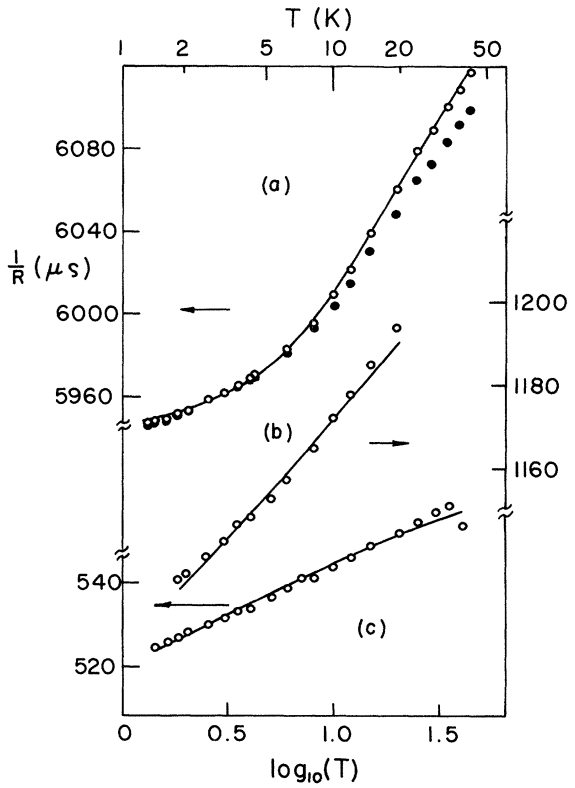

FIG. 8. Resistance of Pd films vs temperature. ○, at 13.5 T; ●, at zero field (uniformly shifted in R). Solid lines are fits using Eq. (17) and parameters of Table I, except for 55-Å film, discussed in Appendix D. (a)=55-Å film, (b)=(30—32)-Å film, and (c)=(6—7)-Å film.

the thinner films. The values of $\bar{\beta}[1-(F/2)]$ are comparable to those derived from the MR. The 55-Å film shows a pronounced curvature which is approximately field independent. Since this occurs only in the thickest film it may be a bulk effect and a possible origin is discussed in Appendix D.

C. Comparison with other experiments

The picture that is emerging in 2D metal films seems relatively clear in its broad outlines: MR is dominated by localization effects while many-electron effects contribute mainly to zero-field resistivity. Bergmann[15] found a negative MR in the light metal Mg for which spin-orbit scattering is weak. By adding submonolayer coverages of Au or Fe he was able to test the HLN predictions about the importance of spin-orbit and magnetic impurity scattering. Several groups[8,9,12] have shown that Cu films also conform to localization theory with stronger spin-orbit scattering for the heavier atom. Pd, being still heavier, lies close to the symplectic limit. Heavier still, Pt would be expected to show MR very similar to Pd. This has been observed by Hoffman *et al.*[14] and by us in smooth Pt films.[46] However, our initial observations[11] were on extremely rough Pt films, which we characterized as islands of Pt joined by a monolayer film. In this limit the MR is quite different, being negative and isotropic. We believe that in this case the MR is dominated by the individual grains and spin-orbit scattering is completely suppressed by the quantum-size effect. We will discuss these results at length in a separate publication.[46]

In many bulk metals magnetic impurities produce effects (the Kondo effect) which can easily be confused with localization—a logarithmic dependence of R on T and a negative MR which scales as H/T. Since Pd has a positive MR which does not scale as H/T, these effects may be readily ruled out. A fuller discussion of experimental results for bulk Pd is given in Appendix D.

V. SUMMARY AND CONCLUSIONS

We have shown that a detailed study of the MR of ultrathin metal films can provide a critical test of the predictions of localization and electron interaction theories of electrical conduction in two dimensions. Both effects contribute to the MR, and we have shown that the present theories explain the magnitude, anisotropy, and temperature dependence of the MR. We have also found certain effects which are not explained by present theory—notably, the pronounced drooping of the MR observed in some samples at low temperatures.

We have further shown that these effects provide a sensitive probe for a number of material parameters not easily measured in other experiments.

Finally, we have found evidence in our (6—7)-Å sample, as well as in the Pt films, that MR may also prove to be a valuable probe of film structure, such as effective metallization depth and film roughness, which are otherwise difficult to quantify.

ACKNOWLEDGMENTS

We would like to thank E. Abrahams, J. Jose, H. Fukuyama, and D. Stone for interesting and useful conversations, L. A. Harris, J. Briant, and D. Skelly for the sputtered samples, B. Brandt and J. Rubin for their hospitality at the Magnetic Laboratory, and A. Aizenshtein for help in the data analysis. This work was supported in part by grants from the Research Corporation and Northeastern University's Research and Scholarship Development Fund. The Francis Bitter National Magnet Laboratory at the Massachusetts Institute of Technology is supported by the National Science Foundation.

APPENDIX A: COMPARISON OF EXPRESSIONS FOR THE MANY-ELECTRON MR

In the orthogonal case, expressions have been derived for both spin[27] and orbital[25,28] effects with Eq. (15) describing spin effect. (The results of Refs. 25 and 28 differ since in Ref. 28 the expressions were evaluated to second order in perturbation theory, while in Ref. 25 third-order corrections are included.) Fukuyama[26] has analyzed the symplectic limit, but does not quote the field dependences, only limiting cases. He finds that the MR saturates at high fields, giving a *total* positive MR,

$$\Delta\sigma=-\frac{\beta F}{2}\ln\left[\frac{\hbar v_F}{4\pi l_e k_B T}\right]. \tag{A1}$$

This value is independent of field orientation, but the field at which the MR saturates depends on orientation. For spin effects, which contribute to both parallel and perpendicular MR, saturation occurs for $g_e\mu_B H \gg k_B T$—the same condition as for Eq. (15) to reach its asymptotic limit. The perpendicular MR has an additional contribution due to orbital effects, which saturates when

$$\frac{\hbar eH}{mc} \gg \left[\frac{hv_F}{l_e E_F}\right] k_B T ,$$

a much lower field. Since the residual resistivity can be written

$$R_0^{-1}=\frac{e^2}{\pi h}\frac{E_F l_e}{\hbar v_F} ,$$

we find $\hbar v_F/l_e E_F = R_0/12.95\ \text{k}\Omega \ll 1$, so the orbital effects saturate at a considerably lower field.

Since the many-electron contribution to the MR is small and we do not have explicit expressions for its field dependence, we are approximating it by Eq. (15). This expression levels off at the same field as the spin effects, but does not saturate at high fields, becoming

$$\Delta\sigma'=-\frac{\beta F}{2}\ln\left[\frac{g_e\mu_B H}{1.3 k_B T}\right]. \tag{A2}$$

For the parameters of Table I, this expression differs from a constant by only 10% for $6 < H < 14$ T. However, the argument of the natural logarithm is $\sim 60/T$, whereas for (A1) it is $\sim(200\text{—}300)/T$. Hence at 2 K, (A2) would predict a 50% smaller MR than (A1). In fitting the data,

this would cause us to choose F about 50% larger than its true value.

APPENDIX B: 2D FERMI VELOCITY

The multiple Fermi surfaces of Pd probably modify the expressions for MR in the same manner as the multiple valleys in Si.[40] In the presence of large interband (s-d) scatterings, expressions such as Eqs. (7)—(9) should be valid with an average value of v_F. For simplicity, we chose $m\bar{v}_F=\hbar\bar{k}_F$, and $\bar{k}_F$ is the rms average of k_F. Then

$$\bar{k}_F^2=\frac{1}{N}\sum_n k_{F_n}^2=\frac{2\pi n_{2D}}{N} ,$$

where $n_{2D}=n_{3D}t$ is the 2D electron density and N is the number of occupied levels. For a metal, we have approximately $N=t/a$, where a is the interatomic distance. Hence $\bar{k}_F=(2\pi n_{3D}a)^{1/2}$, which differs only a little from the 3D expression, if there is one electron per atom, and is exact for a monolayer film.

We note that in this model, the residual conductivity

$$\sigma_0=\frac{e^2}{2\pi h}\sum_n l_e k_{F_n}\simeq\frac{ne^2l_et}{\hbar\bar{k}_F} ,$$

which agrees with the expression in the text if $\hbar\bar{k}_F/ne^2=\rho_\infty l_\infty$. For Pd, $n=1.46\times10^{22}$ cm^{-3}, $a=2.25$ Å, so $\bar{k}=4.54\times10^7$ cm^{-1}, $\bar{v}_F=5.3\times10^7$ cm/sec, and $\hbar\bar{k}_F/ne^2=1.28\times10^5$ Ω Å^2, in reasonable agreement with the experimental[36] $\rho_\infty l_\infty$ considering the simplicity of the one-band approximation.

APPENDIX C: KONDO EFFECT ON LOCALIZATION

We briefly discuss how the Kondo effect will modify the parameter l_s which enters into localization theory. The theory has not been worked out in detail, so our results remain qualitative. The chief result is that even in the high-field and low-T limit, we may expect to find a constant contribution to l_s.

(a) Field dependence. When the magnetic field satisfies $Sg^*\mu_BH\gg k_BT$ (where S is the impurity spin and g^* the impurity g factor) then all of the impurities will be aligned along the field, and spin-flip scattering will be greatly reduced. This can be accounted for in localization theory by making l_s anisotropic, with l_s^z along the field direction and l_s^x perpendicular. In a high field, $(l_s^x)^{-1}\to0$, while l_s^z remains. Reference 24 indicates how to include the anisotropy in the MR, Eqs. (8) and (9). The data of Fig. 4 concern a film close to the symplectic limit, for which the simpler expression, Eq. (5), may be used. In this case it can be shown that $l_s\to3l_s^z$ in the high-field limit. It is important to recognize that the localization effect is produced by spin-flip scattering, but in this case, the spin flip is produced by the spin-orbit interaction. The magnetic impurity scattering interferes with the phase coherence and reduces the magnitude of the MR.

(b) Temperature dependence. At sufficiently low T the localized moments vanish due to the Kondo effect.[47] Hence l_s^{-1} should vanish. In Pd, however, many magnetic impurities[48] (Fe,Co,Mn) have a characteristic temperature considerably below 1 K, so that these effects would not be observable in our T range.

APPENDIX D: RESISTIVITY OF BULK DOPED Pd

A difficulty arises in analyzing metal-film data in terms of localization effects since bulk Kondo effects are also capable of producing negative MR and resistances varying as $\ln T$. Since these are bulk effects, they become progressively less important as the film thickness is reduced,[9] but may produce observable effects in thicker films. We here provide a brief survey of literature results, to see if we can understand the 55-Å film, which shows (Fig. 8) an anomalous, field-independent resistivity with negative temperature coefficient or resistivity (TCR).

Table III lists the characteristics of low T zero-field resistivity for a variety of impurities in Pd. It is seen that a simple Kondo-type result, negative TCR with $\rho\propto\ln T$, is quite rare, except for high impurity concentrations or high T (T_s is typically 40—300 K). Our 55-Å-film data can be fit to form (d) (see Table III), but with a very low value of $T_s=5$ K (Fig. 8). From this fit we obtain the lower limit of $\bar{\beta}(1-F/2)$ listed in Table I; the upper limit is just the fit to the logarithmic slope observed at high T.

The lack of MR for our film still poses a problem, since in the doped Pd, form (d) is accompanied by a negative MR which would eliminate the T dependence at 13.5 T. However, the mechanism producing the negative TCR (for Rh, Ag, and some other *nonmagnetic* impurities) is

TABLE III. Impurity-induced $\rho(T)$ for Pd.

Type	TCR	Behavior of $\rho(T)$	Impurity	References
(a) Electron-electron	+	T^2	pure Pd	
Electron-paramagnon			Ni	49
(b) Dilute ferromagnets	+	$T^{1.5}$ (low T)	Fe, Mn, Co	43
			Cr, 7—14 at. %	48
	+	$\ln T$ (above T_c)	Co	50
(c) In spin-glass regime	−	$\ln T$ ($T<4.2$ K)	Cr, 14—18 at. % (no MR to 4.5 T)	51
(d) Kondo	−	$\ln[(T^2+T_s^2)^{1/2}]$	Cr <7 at. % ($T_s\sim25$—150 K)	48
			V	
Nonmagnetic	−	T^2	Rh(>1 at. %);Ag(20—55 at. %); Pt(~40 at. %),Ru	52

not the ordinary Kondo effect, but a band-structure effect peculiar to Pd. The MR is then produced by ordinary electronic spin splitting. It is likely that, in the presence of strong spin-orbit scattering, this splitting will be quenched and the MR will not be observed—just as we fail to observe the effect of Zeeman splitting on the localization.

For most *magnetic* impurities in Pd, a negative MR is found, which is a function only of H/T. The form is, in fact, very similar to the Lee-Ramakrishnan MR due to interaction, except that (1) the signs are opposite, and (2) in the Kondo system the effective g factor is that of the magnetic impurity, which should be ~ 10. If we refit the MR, but assume the presence of some bulk Kondo-type term, the only parameter which changes is F, which increases to just cancel the Kondo term. For instance, if the 55-Å film contains ~ 1 at. % of Fe, F will be increased to ~ 0.06.

[1]E. Abrahams, P. W. Anderson, D. C. Licciardello, and T. V. Ramakrishnan, Phys. Rev. Lett. 42, 673 (1979); P. W. Anderson, E. Abrahams, and T. V. Ramakrishnan, *ibid.* 43, 718 (1979).

[2]B. L. Altshuler, A. B. Aronov, and P. A. Lee, Phys. Rev. Lett. 44, 1288 (1980); B. L. Altshuler, D. Khmel'nitzkii, A. I. Larkin, and P. A. Lee, Phys. Rev. B 22, 5142 (1980).

[3]S. Hikami, A. I. Larkin, and Y. Nagaoka, Prog. Theor. Phys. 63, 707 (1980).

[4]Y. Kawaguchi and S. Kawaji, J. Phys. Soc. Jpn. 48, 699 (1980).

[5]D. J. Bishop, D. C. Tsui, and R. C. Dynes, Phys. Rev. Lett. 44, 1153 (1980); 46, 360 (1981).

[6]M. J. Uren, R. A. Davies, and M. Pepper, J. Phys. C 13, L985 (1980).

[7]G. J. Dolan and D. D. Osheroff, Phys. Rev. Lett. 43, 721 (1979).

[8]Cu, Cu-Ag, and Cu-Au: F. Komori, S. Kobayashi, Y. Ootuka, and W. Sasaki, J. Phys. Soc. Jpn. 50, 1051 (1981); F. Komori, S. Kobayashi, and W. Sasaki, Surf. Sci. 113, 540 (1982); J. Phys. Soc. Jpn. 51, 3136 (1982).

[9]Cu: L. van den dries, C. Van Haesendonck, Y. Bruynseraede, and G. Deutscher, Phys. Rev. Lett. 46, 565 (1981); C. Van Haesendonck, L. Van den dries, Y. Bruynseraede, and G. Deutscher, Phys. Rev. B 25, 5090 (1982).

[10]Cu: M. E. Gershenson and V. N. Gubankov, Solid State Commun. 41, 33 (1982).

[11]Pt and Pd: R. S. Markiewicz and L. A. Harris, Phys. Rev. Lett. 46, 1149 (1981); Surf. Sci. 113, 531 (1982).

[12]Pd: G. Bergmann, Phys. Rev. Lett. 43, 1357 (1979).

[13]Pd and Pd-Au: W. C. McGinnis, M. J. Burns, R. W. Simon, G. Deutscher, and P. M. Chaikin, Physica 107B, 5 (1981).

[14]Pt: H. Hoffmann, F. Hofmann, and W. Schoepe, Phys. Rev. B 25, 5563 (1982).

[15]Mg, Mg-Fe, and Mg-Au: G. Bergmann, Phys. Rev. B 25, 2937 (1982); Phys. Rev. Lett. 48, 1046 (1982); 49, 162 (1982).

[16]Ni: S. Kobayashi, Y. Ootuka, F. Komori, and W. Sasaki, J. Phys. Soc. Jpn. 51, 689 (1982).

[17]Au: T. Kawaguti and Y. Fujimori, J. Phys. Soc. Jpn. 51, 703 (1982).

[18]In_2O_{3-x}: Z. Ovadyahu, S. Moehlecke, and Y. Imry, Surf. Sci. 113, 544 (1982).

[19]Bi: A. K. Savchenko, V. N. Lutskii, and A. S. Rylik, Zh. Eksp. Teor. Fiz. Pis'ma Red. 34, 367 (1981) [JETP Lett. 34, 349 (1982)].

[20]G. Deutscher and H. Fukuyama, Phys. Rev. B 25, 4298 (1982).

[21]B. L. Al'tschuler and A. G. Aronov, Zh. Eksp. Teor. Fiz. Pis'ma Red. 33, 515 (1981) [JETP Lett. 33, 499 (1981)].

[22]F. J. Dyson, J. Math. Phys. 3, 140 (1962).

[23]E. Abrahams, P. W. Anderson, P. A. Lee, and T. V. Ramakrishnan, Phys. Rev. B 24, 6783 (1981).

[24]S. Maekawa and H. Fukuyama, J. Phys. Soc. Jpn. 50, 2516 (1981).

[25]H. Fukuyama, J. Phys. Soc. Jpn. 50, 3407 (1981); Surf. Sci. 113, 489 (1982).

[26]H. Fukuyama, J. Phys. Soc. Jpn. 51, 1105 (1982).

[27]P. A. Lee and T. V. Ramkrishnan, Phys. Rev. B 26, 4009 (1982); A. Kawabata, Surf. Sci. 113, 527 (1982).

[28]B. L. Al'tschuler, A. G. Aronov, A. I. Larkin, and D. E. Khmel'nitskii, Zh. Eksp. Teor. Fiz. 81, 768 (1981) [Sov. Phys.—JETP 54, 411 (1981)].

[29]A. Houghton, J. R. Senna, and S. C. Ting, Phys. Rev. B 25, 2196 (1982).

[30]L. A. Harris and J. A. Hugo, J. Elchem. Soc. 128, 1203 (1981); L. A. Harris, *ibid.* 129, 2689 (1982).

[31]For example, J. S. Roth and C. R. Crowell, J. Vac. Sci. Technol. 15, 1317 (1978); G. W. Rubloff, P. S. Ho, J. F. Freeouf, and J. E. Lewis, Phys. Rev. B 23, 4183 (1981); R. J. Nemanich, C. C. Tsai, and T. W. Sigmon, *ibid.* 23, 6828 (1981).

[32]T. Narusawa, W. M. Gibson, and A. Hiraki, Phys. Rev. B 24, 4835 (1981); P. S. Ho, P. E. Schmid, and F. Foll, Phys. Rev. Lett. 46, 782 (1981); K. Okuno, T. Ito, M. Iwami, and A. Hiraki, Solid State Commun. 44, 209 (1982).

[33]R. S. Markiewicz, C. J. Rollins, and J. S. Brooks, Surf. Sci. (in press).

[34]H. H. Sample, B. L. Brandt, and L. G. Rubin, Rev. Sci. Instrum. 53, 1129 (1982).

[35]E.g., G. Brandli and J. L. Olsen, Mater. Sci. Eng. 4, 61 (1969).

[36]K. C. Elsom and J. R. Sambles, J. Phys. F 11, 647 (1981). This is similar to Pt [G. Fischer and H. Hoffmann, Solid State Commun. 35, 793 (1980)], although in an earlier study by R. P. Huebener [Phys. Rev. 140, A1834 (1965)] found $\rho_\infty l_\infty = 7\times 10^4\ \Omega\,\text{Å}^2$.

[37]The terms proportional to l_e^2 are negligible for the parameters of Table I.

[38]M. J. Uren, R. A. Davies, M. Kaveh, and M. Pepper, J. Phys. C 14, L395 (1981).

[39]A. I. Larkin, Zh. Eksp. Teor. Fiz. Pis'ma Red. 31, 239 (1980) [JETP Lett. 31, 219 (1980)].

[40]H. Fukuyama, J. Phys. Soc. Jpn. 49, 649 (1980).

[41]R. Meservey and P. M. Tedrow, Phys. Rev. Lett. 41, 805 (1978).

[42]J. S. Dugdale, *Electronic Properties of Metals and Alloys* (Arnold, London, 1977).

[43]G. Williams and J. W. Loram, J. Phys. F 1, 434 (1971), and references therein.

[44]A. D. C. Grassie, G. A. Swallow, G. Williams, and J. W. Loram, Phys. Rev. B 3, 4154 (1971).

[45]Au films are nonconducting if they are ≤ 2 monolayers thick [K. Okuno, T. Ito, M. Iwami, and A. Hiraki, Solid State Commun. 34, 493 (1980)].
[46]R. S. Markiewicz and C. J. Rollins (unpublished).
[47]F. J. Ohkawa, in *Anderson Localization,* edited by Y. Nagaoka and H. Fukuyama (Springer, Berlin, 1982), p. 113; F. J. Ohkawa, H. Fukuyama, and K. Yosida, J. Magn. Magn. Mater. 31, 543 (1983).
[48]R. M. Roshko and G. Williams, J. Magn. Magn. Mater. 20, 71 (1980), and references therein.
[49]A. I. Schindler and M. J. Rice, Phys. Rev. 164, 759 (1967).
[50]J. W. Loram, G. Williams, and G. A. Swallow, Phys. Rev. B 3, 3060 (1971).
[51]R. W. Cochrane, J. O. Strom-Olsen, and G. Williams, J. Phys. F 9, 1165 (1979).
[52]J. A. Rowlands and S. B. Woods, Phys. Rev. B 6, 1162 (1972).